PHYSICAL REVIEW B VOLUME 27, NUMBER 5 1 MARCH 1983

$Z(4)$ model on the triangular lattice

Yoel Stavans and Eytan Domany
Department of Electronics, The Weizmann Institute of Science, Rehovot, Israel
(Received 21 June 1982)

Monte Carlo studies of the $Z(4)$ (or Ashkin-Teller) model on the triangular lattice were carried out. In particular, we investigated whether the massless phase, which was shown to exist on the boundary of the physical parameter space, may extend into a region of finite width. The existence of such a phase would imply that N_c, the critical value above which $Z(N)$ models have intermediate phases, is nonuniversal, i.e., lattice and interaction dependent. Although, on the basis of our Monte Carlo results we cannot completely rule out this possibility, most aspects of our findings indicate consistency with existing theories of the $Z(4)$ model which exclude the possibility of such an intermediate massless phase.

I. INTRODUCTION

The critical properties and phases of various models in two dimensions are the subject of numerous investigations.[1] In particular, the XY model in the presence of N-fold-symmetry-breaking fields[2] h_N, and its discrete version, the $Z(N)$ models,[2,3] are of both theoretical interest and experimental relevance.[4]

Consider the Hamiltonian

$$H\{\theta\}=\sum_{\langle i,j\rangle} V(\theta_i-\theta_j)-h_N\sum_i \cos(N\theta_i)\ , \quad (1.1)$$

where $-\pi<\theta_i<\pi$ is an angle associated with site i, and the nearest-neighbor ferromagnetic interaction term $V(\theta)$ is a periodic, even function

$$V(\theta)=V(\theta+2\pi)=V(-\theta)\leq V(0)\ . \quad (1.2)$$

For $h_N=0$ the model exhibits at low temperatures a massless phase.[5] For $h_N\to\infty$, an N-state discrete model is obtained.

José *et al.*[2] have studied the model (1.1) with the Villain form of the interaction $V(\theta)$. They have shown that the critical behavior of this model with $h_N=0$ is governed by the Gaussian line of fixed points, and they have analyzed the stability of this line with respect to small h_N perturbations. They found h_N to be relevant for temperatures $T<T_1(N)$ and irrelevant for $T>T_1(N)$. They also found that for $N<4$, $T_1(N)>T_{\rm KT}$, (where KT stands for Kosterlitz and Thouless), the temperature at which the Gaussian line becomes unstable to vortex excitation, while for $N>4$, $T_1(N)<T_{\rm KT}$. Therefore, they predict that the XY model will, in the presence of *small h_N perturbations,* exhibit an intermediate massless phase for $N>4$. For the case $N=4$ no massless phase is predicted to exist.

They have also shown that the discrete $Z(N)$ model with the Villain interaction is self-dual; that is, the dual model also has the Villain form. This relationship, together with Griffiths-type inequalities, was used by Elitzur, Pearson, and Shigemitsu,[3] who have shown that for $N>N_c$ the $Z(N)$ model with the Villain interaction has an intermediate massless phase. They estimate $N_c\geq 4$; however, no exact derivation of N_c exists nor has the question of the universality of N_c been rigorously resolved.

In this paper we study whether N_c may depend on the lattice on which the model is defined, and on the particular interaction $V(\theta)$ chosen. To address this issue, we have performed Monte Carlo studies of the $Z(4)$ model on the triangular and square lattices.

Renormalization-group (RG) arguments[6–9] indicate that for $N=4$ no massless phase should occur, independently of the lattice and the shape of the nearest-neighbor interaction potential. Some of the arguments leading to this conclusion, and the widely accepted fixed-point structure of the model, are briefly discussed in Sec. II. A simple argument[10] that proves the existence of a massless phase on the boundary of the physical region for the triangular lattice is also reviewed. If this "massless phase" does extend into the physical region of the $Z(4)$-model parameter space, this would indicate that the commonly accepted picture has some serious flaws.

Our numerical results for the triangular lattice are presented in Sec. III; where needed, comparison with results obtained for the square lattice is also given. Section IV summarizes our findings.

II. THE Z(4) MODEL—A SHORT REVIEW

As shown by Fan[11] the $Z(4)$ (or Ashkin-Teller) model can be regarded as composed of two interacting Ising models defined on the same two-dimensional lattice. Denoting by s_i and t_i the Ising variables on site i, the Hamiltonian of the $Z(4)$ model is given by

$$\tilde{H}=\frac{H}{k_BT}=\sum_{\langle i,j\rangle}(K_1s_is_j+K_2t_it_j)+L\sum_{\langle i,j\rangle}s_is_jt_it_j\ . \tag{2.1}$$

We concentrate here on the case $K_1=K_2=K$. Notice that for $L=0$ the Ising models are decoupled whereas for $K=L$ the four-state Potts model is obtained. The $Z(4)$ model can be parametrized conveniently by the Boltzmann factors:

$$X(90)=\exp[-2(K+L)]\ ,\qquad X(180)=\exp[-4K]\ . \tag{2.2}$$

The physical region corresponds to the square $0\le X(90),X(180)\le 1$. For any particular interaction (i.e., any specific value of the ratio K/L), variation of temperature defines a trajectory in this square that connects the zero-temperature point $X(90)=X(90)=0$ with the infinite temperature one $X(90)=X(180)=1$. In the regime $X(90)<X(180)$, the model exhibits two Ising transitions with an intermediate partially ordered phase. For $X(90)>X(180)$, a line of continuously varying critical exponents is observed whose nature can be elucidated by performing a duality transformation on one of the two Ising variables. It turns out[12] that a staggered eight-vertex model, believed to have continuously varying critical indices, is obtained [the nonstaggered eight-vertex (8V) model was solved exactly by Baxter].[13] This fact suggested possible connections between the critical exponents of both models. These connections were obtained by various workers using different methods. Kadanoff and Brown[6] applied a universality argument describing the relation between the correlation functions of both models and the known correlations of the Gaussian model. They noted first that at the decoupling points of the $Z(4)$ and 8V models, many correlation functions have the same asymptotic form as the correlation functions of the Gaussian model with a coupling $\tilde{K}=1/\pi$. Second, they showed that this holds true as well for other points on the critical lines of both models, and calculated explicitly the functions $F_{8V}(\tilde{K})$ $[F_{Z(4)}(\tilde{K})]$, which give, for each value of the Gaussian coupling $\tilde{K}$, the point on the critical line of the 8V $[Z(4)]$ model at which the correlation functions should be compared. Since these functions render critical Hamiltonians, an operator product expansion could be calculated, thereby allowing the authors to obtain the variation of the critical indices in the vicinity of the decoupling points along the respective critical lines of both models. Kadanoff[7] pointed out, however, that their conclusions could break down with the appearance of an additional marginal operator whose existence they could not rule out.

Knops[8] employed renormalization-group techniques and studied a generalized Villain model which contains the 8V model as a particular case. He showed that the correspondence between 8V and Gaussian operators found in Ref. 6 was indeed an equivalence under renormalization, and that this equivalence breaks down when below a certain coupling, the Gaussian model is repelling for trajectories departing from the 8V model. This is equivalent to the appearance of new marginal operators as found in Refs. 6 and 7. Of course, this carries on as well for the $Z(4)$ model. Knops and den Ouden[9] have recently extended this approach and obtained more operator equivalences between the models.

den Nijs[14] constructed a mapping between the 8V model and a one-dimensional quantum theory of massless fermions (the Luttinger model) which is integrable in the continuum limit as shown by Mattis and Lieb.[15] The Luttinger model is a quantum version of the Gaussian model. In the mapping process he identified spin-wave and vortex operators in the 8V model with a corresponding set of fermion operators in the Luttinger model. By computing correlation functions between these fermion operators, den Nijs obtained the same relations between the critical indices of both models as obtained in Refs. 6 and 8.

The above statements hold for the critical line of the $Z(4)$ model. We now consider a different line, e.g., $X(180)=0$, and show that for the $Z(4)$ model on a triangular lattice it is of particular interest. It is found[16] that in the case of a triangular lattice a massless phase occupies a finite portion of this line, whereas for a square lattice no such phase is expected. The equivalence of the $Z(4)$ model on a triangular lattice, with $X(180)=0$, to a solid-on-solid (SOS) and XY model, has been presented elsewhere.[16] Nevertheless, we proceed to give a proof, for completeness sake, along the same lines as has been previously done for the $Z(5)$ model on a square lat-

tice.[10]

Consider the low-temperature series for the $Z(4)$ model on the line $X(180)=0$ for the triangular lattice. Any allowed state is characterized by integers $\{n_i\}$ associated with site i, with $n_i=1,2,3,4$ (corresponding to $\theta_i=\pi n_i/2$), such that nearest-neighbor pair (ij) cannot have $|n_i-n_j|=2$. For any given $\{n_i\}$ configuration assign arrows to the bonds, pointing from low to high n value, with the convention that if $n_i=4$ and $n_j=1$, the arrow points from i to j, and if $n_i=n_j$, no arrow is assigned. The allowed arrow configurations for a basic up-pointing triangle are shown in Fig. 1(a). Each configuration $\{n_i\}$ defines an allowed arrow configuration. To identify the allowed graphs, rotate each edge clockwise by 90°. The rotated edges form now a honeycomb lattice, with vortices that can have either no arrows on the incident edges, or one incoming and one outgoing arrow [Fig. 1(b)]. Thus each allowed $\{n_i\}$ configuration on the triangular lattice defines an allowed graph, consisting of closed nonintersecting polygons on the honeycomb lattice. Each polygon can have either clockwise or anticlockwise oriented arrows. The partition function is given by[16]

$$Z=\sum_G W(G)W_1^{L(G)}2^{n(G)}, \tag{2.3}$$

where G is an allowed graph with a total of $L(G)$ arrows and $n(G)$ disconnected closed polygons. $W(G)$ is the number of ways the graph G can be embedded in the lattice and the factor $2^{n(G)}$ appears due to the two possible arrow orientations of each polygon. W_1 is the Boltzmann weight for

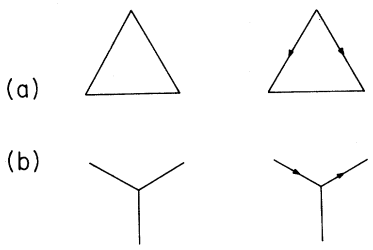

FIG. 1. (a) Allowed arrow configurations for each elementary up-pointing triangle in the lattice. An arrow represents a bond joining two sites for which the order parameter $\theta_i=\pi n_i/2$ differs by ± 90 (or $|n_i-n_j|=1$). The arrow points from low to high n. When no arrow is present, the variable at both sides of the bond has the same value. The diagram with two arrows also represents two other configurations obtained from the one shown by rotating the triangle by 120° and 240°. (b) Allowed vertex configurations corresponding to each arrow configuration in (a).

$|n_i-n_j|=1$.

Consider now the solid-on-solid model defined in terms of integers $\{h_i\}$ associated with each site i of a triangular lattice; $\infty<h_i<\infty$. Choose the interaction

$$\exp[-V(h_i-h_j)]=\begin{cases}1, & h_i=h_j\\ W_1, & |h_i-h_j|=1\\ 0, & \text{otherwise}.\end{cases} \tag{2.4}$$

To obtain an expression for the partition sum Z, repeat the preceding procedure; assign arrows to bonds with $|h_i-h_j|=1$, pointing from low to high value of h_i (h_j). Again the same allowed graphs G appear as in Fig. 1(a), and Z is given by (2.3). Since this SOS model has a roughening transition for $W_1>W_c$, one expects a massless phase (i.e., divergent correlation length ξ) for the $Z(4)$ model on the line $X(180)=0$ as well.

The reason that allowed us to construct a mapping between the line $X(180)=0$ and the SOS model is the fact that on this special line no $Z(4)$ vortices are allowed to appear. On the other hand, vortex configurations are allowed when the model is defined on a square lattice, so a similar mapping cannot be constructed. We therefore do not expect to find a massless phase on this line for the square-lattice case. It is possible that as soon as $X(180)>0$, the massless phase disappears and ξ is finite. On the other hand, if the massless phase extends into the physical $(X(90),X(180))$ plane, as in the case of the $Z(5)$ model on a square lattice, the consequences are quite far reaching. If so one can choose $V(\theta)$ in (1.1) in such a way that as the temperature is varied, the model traces a trajectory from $T=0$, $X(90)=X(180)=0$, to $T=\infty$, $X(90)=X(180)=1$, along which three phases occur: a paramagnetic phase, a phase with long-range order, and an intermediate massless phase. If such is the case, this means that the critical value N_c (beyond which a discrete N-state clock model has an intermediate massless phase) is nonuniversal, that is, lattice dependent. Furthermore, for a given lattice, then, N_c depends on the particular interaction $V(\theta)$ chosen.

The question of whether there are three phases for $X(90)>X(180)$ (i.e., an intermediate massless phase bounded by ordered and disordered phases) has been addressed by many authors. Elitzur *et al.*,[3] Einhorn *et al.*,[17] and Alcaraz and Koberle[18] have taken advantage of the self-duality of the $Z(4)$ Villain model when defined on a square lattice, and have concluded that only two phases occur for

$X(90) > X(180)$ in agreement with the phase diagram we have described above. The line of varying critical indices is in fact a self-dual line.

Savit[19] has analyzed two types of $Z(N)$ Villain models on a triangular lattice. In the first version the vortices occupy half the sites of the honeycomb lattice dual to the original triangular one (T_h model). In the second, the vortices occupy half the sites of the honeycomb lattice forming themselves a triangular lattice (T_t model). Savit claimed that these two models belong to the same universality class as the $Z(N)$ Villain model on a square lattice. Since the T_t model is self-dual, he applied the same reasonings as Elitzur *et al.*[3] to prove the inconsistency of a three-phase picture for $N < N_c = 5$. Savit's conjecture that the T_t and T_h models belong to the same universality class was based on the similarity of both theories, differing only on the lattice structure of their vortices. No rigorous justification was given. Nevertheless, Savit's result agrees with the common belief, based on grounds of universality, that the model has the same phase structure, independently of the lattice on which it is defined.

In contrast to the square-lattice case, the line of varying critical exponents found for the triangular lattice is not a self-dual line since the model itself is not self-dual. Enting,[20] however, has calculated a special line by applying a star-triangle transformation to the dual model which is defined on a honeycomb lattice. He has shown, that on this line the three-site interactions (generated by the star-triangle transformation) vanish; each point on this line maps onto itself by the duality followed by star-triangle transformation. The equation of this line is

$$2X^2(90)[1+X(180)]+X^2(180)=1\ , \qquad (2.5)$$

and Enting conjectures that for $X(90) \geq X(180)$ this is where the transition occurs. For $X(180)=0$ the critical value[21] of $X(90)=1/\sqrt{2}$ is obtained.

At this point it will be convenient to consider the renormalization-group picture of José *et al.*[2] and Kadanoff[7] which connects the $Z(4)$ model with the XY and Gaussian models. José *et al.*[2] analyzed a generalized Villain model with symmetry-breaking interactions. In the model, vortices were controlled by a chemical potential y_0 and symmetry-breaking excitations by y_N. The stability of the Gaussian line under both kinds of perturbations for the specific case $N=4$ is depicted in Fig. 2. Their RG analysis indicated the presence of three lines of fixed points, i.e., the Gaussian and $y_0 = \pm y_4$ lines intersecting at the transition point of the XY model.

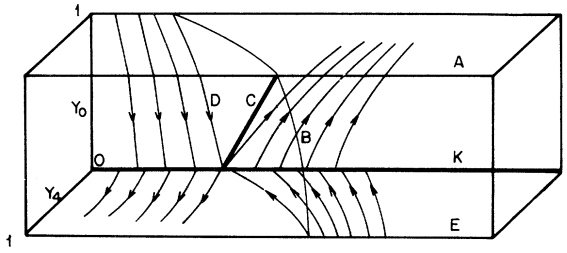

FIG. 2. Parameter space of the generalized Villain model (Ref. 2) (with vortex fugacity y_0 and four-fold-symmetry-breaking y_4), defined on a *triangular lattice.* The Gaussian line K and line C are two of the three lines of fixed points identified by the renormalization group analysis of José *et al.* C is the sink of the critical manifold spanned by D,C,B. The parameter space of the $Z(4)$ model intersects the $y_4=1$ plane on the Villain line and the SOS line E. For the $Z(4)$ model on the square lattice, the line E is not in the $(X(90),X(180))$ parameter space.

The plane $y_4=1$ corresponds to an infinite symmetry-breaking field, thus on this plane the order parameter is restricted to take only four possible directions. On this plane there must be a line of transitions corresponding to the $Z(4)$ line of varying critical exponents (line B). Furthermore, the line $y_0=y_4=1$ (line A) corresponds to the Villain form of the interaction. The lines B,C,D lie on a critical manifold. Under application of RG transformations, the points of this critical manifold are attracted to the line of fixed points C. It must be pointed out, however, that the analysis of José *et al.* was done in the vicinity of the Gaussian line and amounts to an expansion in the small parameters y_0 and y_4. Therefore, the flows, the stability, and the nature of the fixed lines are correct only in the neighborhood of the multicritical point. Thus the intersection of line C with the $Z(4)$ plane as depicted in Fig. 2 is based on various conjectures.[8]

The conclusions reached by José *et al.*[2] are not altered if the cosine interaction is used instead of the Villain form; Amit *et al.*[22] have proved that the more severe nonlinearities inherent in the cosine interaction, which do not permit the factorization of the partition function into spin-wave and vortex parts, are irrelevant near the Gaussian limit.

The connection between this RG picture and the parameter space $[X(90),X(180)]$ can be described as follows: Suppose we define a general Hamiltonian for the $Z(4)$ model containing the parameters $X(90),X(180)$ and in addition a plaquette interaction with Boltzmann weight XP which in some way contols the vorticity. The three-dimensional space

$(X(90),X(180),XP)$ contains then the $Z(4)$ plane ($y_4=1$) of Fig. 2, as well as the $(X(90),X(180))$ plane. These two planes intersect at the line corresponding to the Villain form of the interaction [line A in Fig. 2, and a corresponding trajectory in the $(X(90),X(180))$ plane (line V) with a specific value of the ratio K/L, see Fig. 9].

In order to understand how the existence of the massless phase on the $X(180)=0$ line of the triangular lattice fits into this picture, the following should be noted. On this special line, the $Z(4)$ model does not allow vortices; therefore, this line can be identified with the line E, e.g., $y_4=1$, $y_0=0$ of Fig. 2. Indeed, a section (corresponding to high temperatures) of line E flows under the RG transformation, onto *the high-temperature* section of the Gaussian line. Therefore, according to the above presented (commonly accepted) picture, as soon as $y_0\neq 0$, [or $X(180)>0$] the massless phase should disappear. It is this aspect of the $Z(4)$ model in the triangular lattice that we have set out to investigate.

III. RESULTS

We performed Monte Carlo (MC) simulations of the Fan version [see Eq. (2.1)] of the $Z(4)$ model by the standard Metropolis method. The $Z(4)$ variable at each site was updated sequentially. In order to speed up convergence, a parameter p controlling the relative probability of flipping the variable by 180° (i.e., flipping both Ising variables) versus the probability of flipping it by $\pm 90°$ was introduced. We found that our results were almost insensitive to the value of p, and generally the value $p=\frac{2}{3}$, which assigns equal probability to each of the three possible directions was used. Reliability of the results was established by comparing the values of the physical quantities calculated on the basis of independent MC sequences. Typically each site was visited 11.000 times during a single MC sequence. In order to ensure independence of the results of the initial configuration chosen, about 10% of the generated configurations in the beginning of each Markov chain were not taken into account in the computation of the quantities of interest. The following thermodynamic averages were calculated:

(a) the specific heat per spin,

$$\frac{C}{k_B N^2}=\langle \tilde{H}^2\rangle-\langle \tilde{H}\rangle^2 , \tag{3.1}$$

where $\tilde{H}$ is the reduced Hamiltonian given by Eq. (2.1).

(b) the susceptibilities per spin in the x and y directions,

$$\frac{k_B T\chi_{ii}}{N^2}=\frac{1}{N^2}[\langle \sum_{l,m} s_i^l s_i^m\rangle-\langle(\sum_l s_i^l)^2\rangle] , \tag{3.2}$$

where s_i^l is the ith component ($i=x,y$) of the $Z(4)$ variable s^l at site l.

These quantities were calculated as a function of temperature, for various trajectories in the $[X(90),X(180)]$ plane. A trajectory is defined by

$$[X(90),X(180)]=(X_0^{1/T},Y_0^{1/T}) , \tag{3.3}$$

thus all trajectories extend from (0,0) to (1,1), as $0<T<\infty$. For each plot the coordinates (X_0,Y_0) are specified.

The region to be probed is the $X(90)>X(180)$ sector in which a single transition is expected. The specific heat for various trajectories in this sector is shown in Fig. 3. For temperature trajectories that pass between the decoupling $[X(180)=X(90)^2]$ and the SOS $[X(180)=0]$ lines, the calculations show the presence of two peaks; for trajectories passing near the point $(X(90),X(180))=(0.9,0.1)$ the low-temperature peak is very sharp and the other one very wide. Neither of the peaks scales with the size of the system. As the decoupling line is approached, the peaks approach one another until they coalesce into a single one, which corresponds to the decoupled Ising models. At the decoupling point the specific heat scales with the size of the system as $C_{\max}\sim \ln N$, in agreement with finite-size scaling theory.[23]

Although we see some growth as the lattice size is increased even before the decoupling line is reached, a plot of the specific-heat maxima as a function of $\ln N$ bends down indicating that from a certain size on no growth is observed; the specific heat saturates. No results are shown in the figure for trajectories between the Potts and decoupling lines. In this region the specific heat exhibits only one peak which scales with the size of the lattice according to $C_{\max}\sim n^{\alpha}$, with $\alpha>0$.

For the SOS line we observe only one peak which does not scale, as expected for an infinite-order transition. It should be noted that for trajectories between the decoupling and SOS lines, the expected transition temperature as given by Eq. (2.5) lies *between* the two specific-heat peaks. The expected transition point is indicated on the temperature axis of each plot. The specific-heat maxima approach these values of T_c as the decoupling line is approached; for trajectories between the decoupling

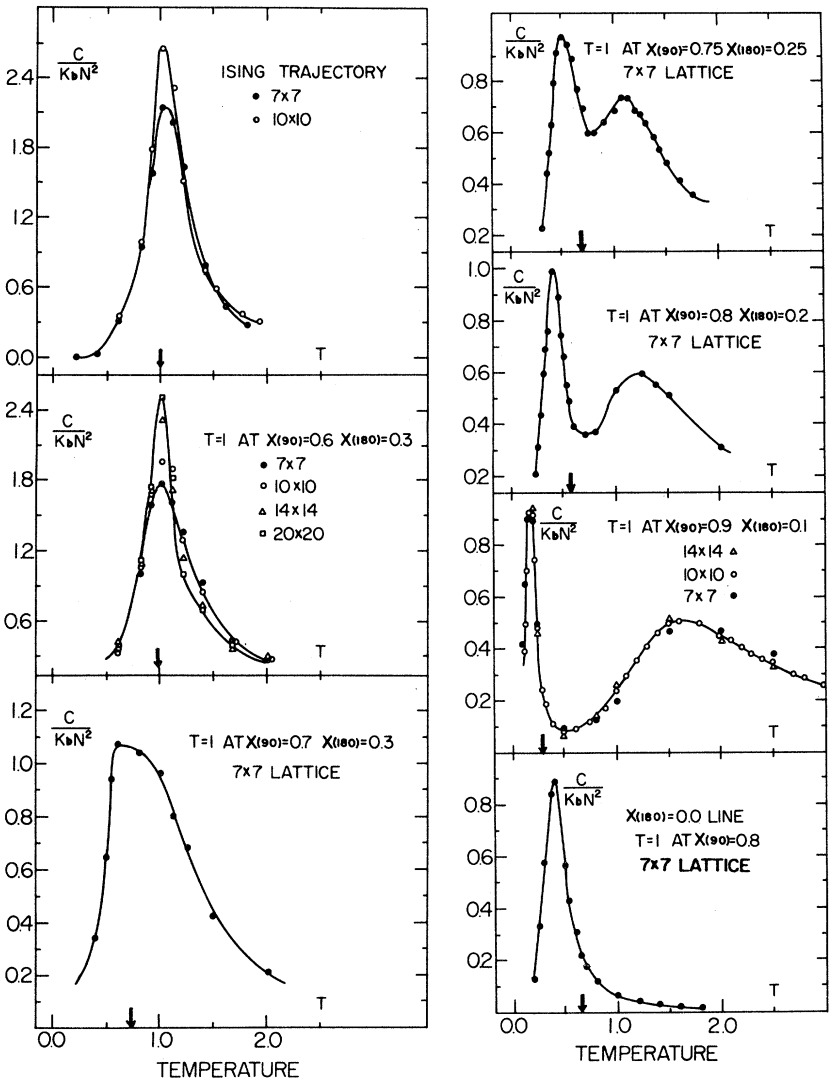

FIG. 3. Specific heat per spin as a function of temperature for various trajectories [defined by Eq. (3.3)] in the $X(90) > X(180)$ sector for the triangular lattice. The point (x_0,y_0) on each trajectory, at which the temperature is normalized to unity, is specified on each figure. The arrow on the temperature axis specifies the temperature at which the particular trajectory intersects the Enting line. The solid lines are guides to the eye.

and four-state Potts lines, the observed (single) maximum does coincide with T_c.

These results were compared with those obtained for a *square lattice.* For the square lattice the specific heat also exhibits two peaks for trajectories below the decoupling line; but the narrow, low-temperature peak closely follows the (self-dual) transition line (see Fig. 4).

Our results for the susceptibility are shown in Fig. 5. On the SOS line we see a high-temperature phase in which the susceptibility scales, indicating the presence of a massless phase as expected (the SOS model is dual to an XY model and therefore the massless phase appears above the transition). As can be seen in the figure, it is very hard to ascertain whether a finite region with massless behavior exists as we leave the SOS line. The decay (if any) in the susceptibility in the region above the transition is very weak for trajectories sufficiently near the SOS line, as exemplified by the line passing through the point (0.9,0.1); the system sizes we studied do not allow us to conclude whether scaling with size will saturate or not in the region in question.

This is not the case for trajectories far from the SOS line and approaching the decoupling point.

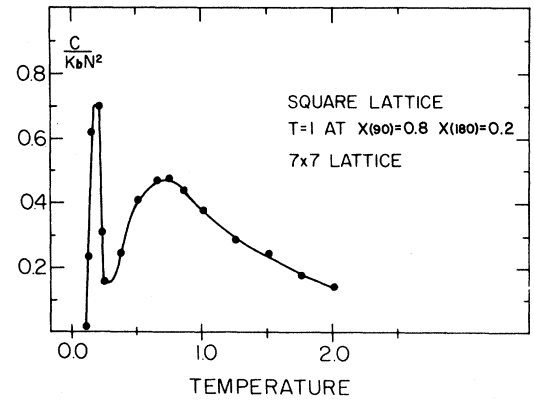

FIG. 4. Specific heat per spin as a function of temperature for a square lattice. The normalization of the temperature is specified in the figure. The maximum of the low-temperature peak coincides within the computational error with the point at which the trajectory crosses the self-dual line. Simulation of a 10×10 system (not shown in the figure) yields the same curve. The solid line is a guide to the eye.

Here it is clear that no scaling region exists after the transition and the peaks are sharper and sharper as the decoupling trajectory is approached.

In order to obtain further information concerning the question of whether the massless phase penetrates into the phase diagram or not, additional runs, with fixed $X(90)$ and varying $X(180)$, were made for $X(90)\geq 1/\sqrt{2}$ (the transition point of the SOS model). The results are shown in Fig. 6. A complete flattening of the susceptibility near the SOS line [as the one observed in Fig. 5, for $X(180)=0$] is not observed. The results indicate that the width [in terms of $X(180)$, near $X(180)=0$] of the region where scaling seems to occur shrinks with increasing lattice size. The width of this crossover region increases as the $X(90)$ coordinate decreases towards $X(90)=1/\sqrt{2}$.

A similar calculation for the square lattice yields the results of Fig. 7. As the $X(180)=0$ line is approached with fixed $X(90)$, we see a small change for the two sizes shown but presumably there is no change at all for larger lattices. This is borne out by the results of Fig. 8. In this figure, the dependence of the susceptibility on N is calculated for different points on the $X(180)=0$ line, for the square and triangular lattices. From finite size scaling we know that the dependence of the susceptibility on N in the case of the SOS model is of the form $N^{2-\eta}$. Therefore, a plot of $\ln\chi$ vs $\ln N$ should yield a straight line with slope $2-\eta$. For the triangular lattice this is indeed the case for $X(90)\geq 0.7$. For $X(90)\leq 0.7$ the points obtained deviate drastically from a straight line even for small lattices, and therefore are not plotted in the figure.

In the case of the square lattice, the curve obtained shows that $\chi(N)$ saturates, indicating clearly that no massless phase exists on this line. In order to check the precise influence of the vortices on the behavior of the model on this lattice, we made some runs at the same point but restricting the MC routine to probe only configurations within the zero vorticity sector of the phase space. The results, depicted in the same figure, show a straight line, as in the triangular case.

The susceptibility data of Fig. 5 for the triangular lattice show a sharp peak at the low-temperature boundary of the apparent scaling region. This peaks follows closely the critical line of Eq. (2.5); the positions [in the $X(90), X(180)$ plane] of this peak as well as the specific-heat maxima are shown in Fig. 9.

IV. DISCUSSION AND SUMMARY

From the results we have presented, we can see marked differences in the behavior of the $Z(4)$ model when defined on a square or on a triangular lattice, although no conclusive evidence for a three-phase picture was found in the latter case. The scaling behavior of the specific heat in both cases is in accord with the accepted theoretical picture. Between the Potts and decoupling trajectories the specific heat scales, indicating that in this sector $\alpha>0$, as expected (α is $\frac{2}{3}$ for the four-state Potts model and 0 for the Ising model). Between the decoupling and $X(180)=0$ lines the specific heat does not scale with the size of the system; therefore we conclude that $\alpha<0$ in this sector.

However, we find the appearance of two peaks in the specific heat intriguing. These appear for trajectories lying between the decoupling and $X(180)=0$ lines, but not between the Potts and decoupling lines. In the latter region the energy fluctuations manifest themselves fully in the divergence of the specific heat, whereas in the other sector this divergence is suppressed and the fluctuations manifest themselves in a narrow peak and a broader one at higher temperatures, both of which do not scale. In the square-lattice case, in which the model is self-dual, the sharp low-temperature peak is observed to follow the self-dual line even for small lattices such as 7×7, allowing us to associate it with the transition. We believe the broad high-

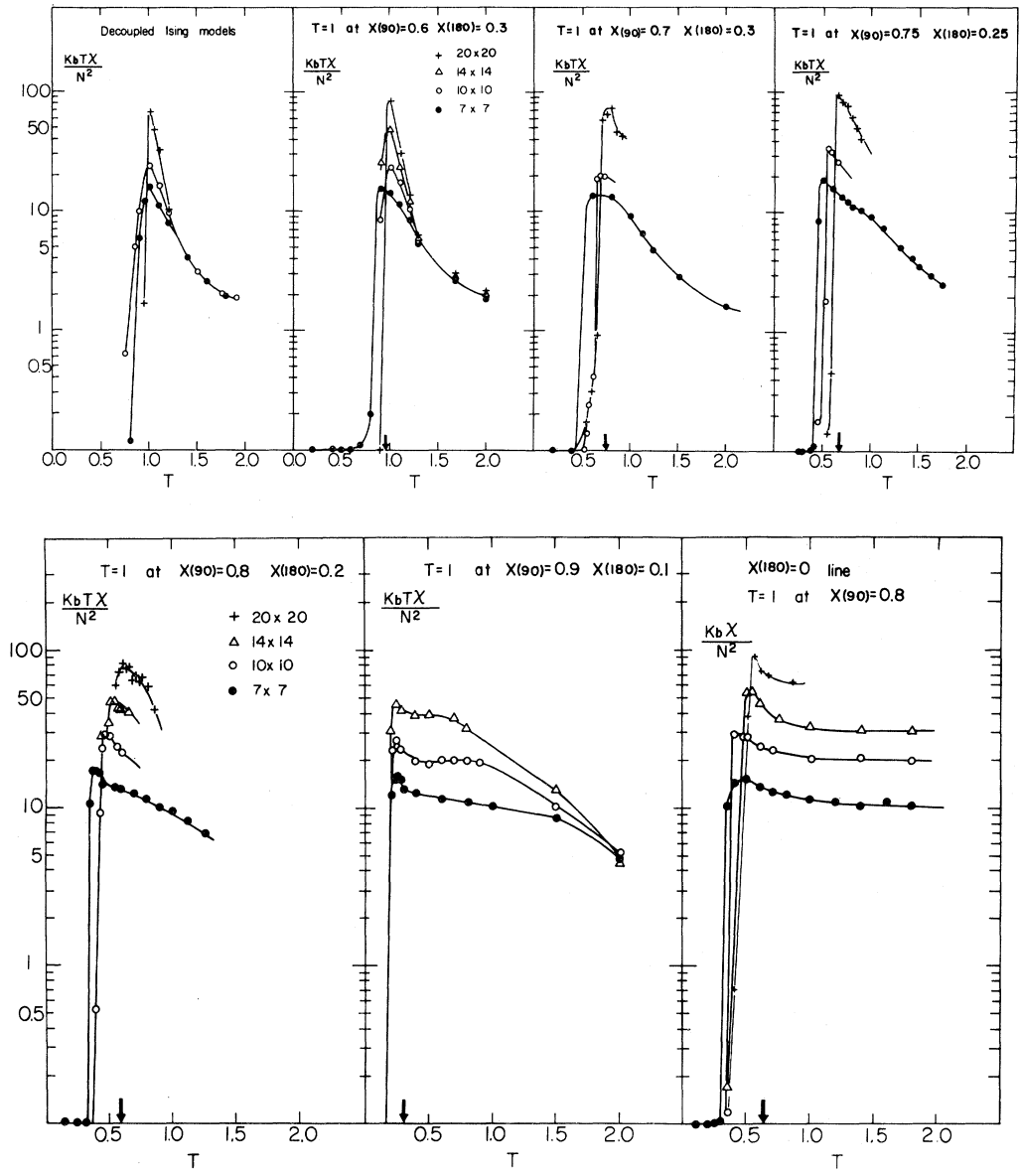

FIG. 5. Susceptibility per spin as a function of temperature for various trajectories [see Eq. (3.3)] in the $X(90) > X(180)$ sector for the triangular lattice. The point (x_0, y_0) on each trajectory at which the temperature is normalized to unity is specified in each case. The arrow on the temperature axis specifies the temperature at which the particular trajectory intersects the Enting line. The solid lines are guides to the eye.

temperature peak represents a region of short-range order.

The location of the specific-heat maxima on the phase diagram for the triangular case is depicted in Fig. 9. The two lines of maxima in the region between the decoupling and SOS lines join at the critical point of the decoupling line and neither of them falls on the line calculated by Enting (line E). This behavior persists for all the lattice sizes for which we made runs (up to a 20×20 lattice). For trajectories between the Potts and the decoupling line, the maximum of the specific heat falls on line E.

The most dramatic difference between the behavior of the model when defined on a triangular versus square is shown by the susceptibility. For the triangular lattice, the susceptibility decreases for temperatures above the transition at a rate that gets slower as the trajectory approaches the SOS line.

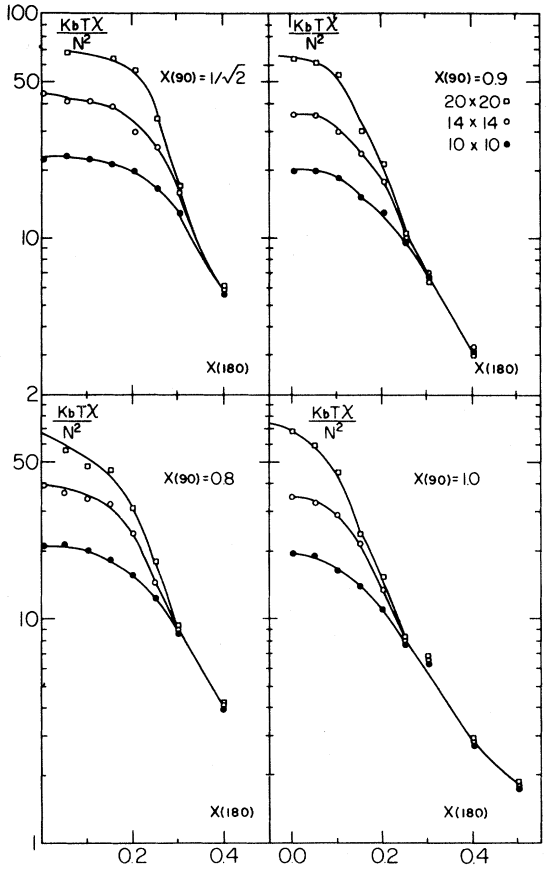

FIG. 6. Susceptibility per spin for fixed $X(90)$ as a function of the Boltzmann weight $X(180)$, for the triangular lattice. The value of $X(90)$ is specified in each case. The solid lines are guides to the eye.

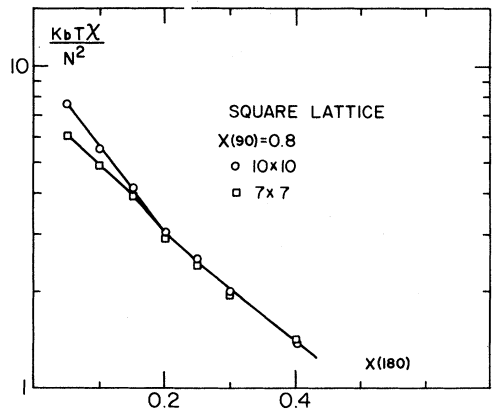

FIG. 7. Susceptibility per spin, for $X(90)=0.8$, as a function of the Boltzmann weight $X(180)$, for the square lattice. No appreciable scaling is observed in this case and the value of the susceptibility near the $X(180)=0$ line is small as compared to the corresponding value for the triangular lattice. The solid lines are guides to the eye.

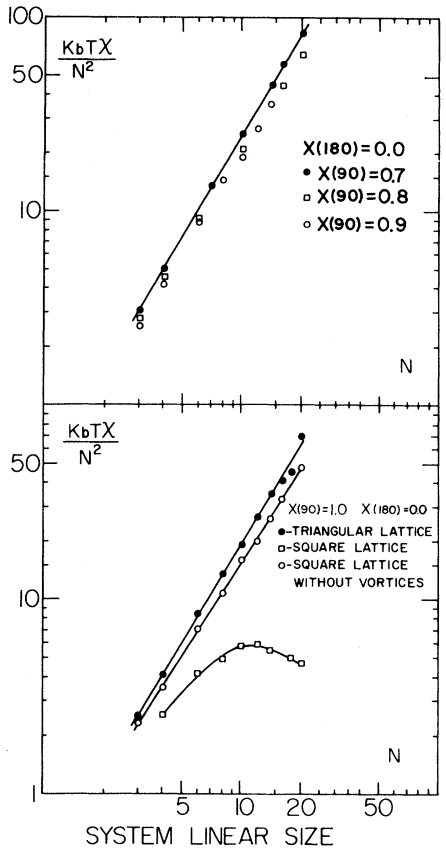

FIG. 8. Dependence of the susceptibility per spin on the linear size of the system for the $X(180)=0$ line. In the upper figure the results for the triangular lattice are plotted for different values of $X(90)$ on the SOS line. Below $X(90)=0.7$, no scaling with size was observed. In the lower figure a comparison is drawn between the behavior of the model on a triangular lattice, a square lattice, and a square lattice without vortices at the same point of the $X(180)=0$ line. For a square lattice we see saturation indicating that no massless phase is present. The solid lines are guides to the eye.

Although studies of larger systems would be desired, our findings indicate that off the SOS line the susceptibility does not exhibit scaling with the size of the system over a region of finite extent, in spite of the considerable flatness seen near the SOS line. Furthermore, the width of the apparent scaling region of χ seems to decrease as the lattice size is increased. This supports the two-phase picture of the model. It is found that the temperature associated with the maximum of the susceptibility changes as the lattice size is increased. We find that the maximum of the susceptibility occurs close to the Enting line for a 20×20 lattice; for smaller sizes the maximum deviates from this line. The ap-

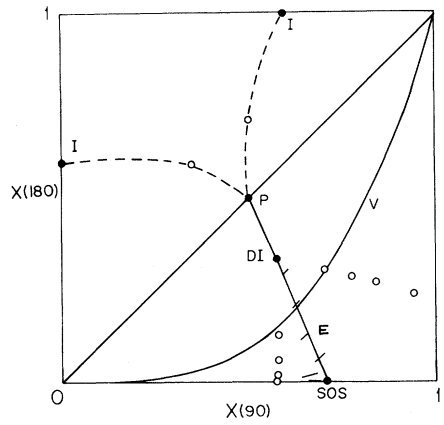

FIG. 9. Phase diagram of the $Z(4)$ model on a triangular lattice. Line V represents the Villain trajectory, P is the critical point on the four-state Potts trajectory, and DI is the critical point of the decoupling line. The point SOS is the critical point of the equivalent SOS model on the $X(180)=0$ line. The Enting line (line E) passes through P, DI, and SOS. The open circles represent the approximate location of the specific heat maxima for different trajectories. In the $X(90)>X(180)$ sector two lines of maxima join at the point DI. The bars represent the approximate location of the susceptibility maxima for different trajectories for a 20×20 system. The dashed lines in the $X(180)>X(90)$ section represent two Ising transitions. These lines end up on the $X(90)=0$ and $X(180)=1$ lines at which the $Z(4)$ model behaves as an Ising model.

proximate location of the susceptibility maxima for a 20×20 lattice is depicted by bars near the Enting line in Fig. 9 for different trajectories. This stands in sharp contrast to the square-lattice case where for a 7×7 lattice we already see the maxima very near the self-dual line. Our results then indicate that the transition takes place on the Enting line. It is puzzling, however, that the low-temperature peak of the specific heat does not coincide in location with the transition temperature as in the case for the square lattice.

The data presented in Figs. 5 and 8 strongly support the fact that the $X(180)=0$ line for the triangular lattice has a massless phase. The clearcut scaling behavior shown in these figures is not observed, however, when the $Z(4)$ model is defined on the square lattice (Figs. 7 and 8). We therefore conclude that no massless phase exists on the $X(180)=0$ line in this case. We also demonstrated the specific role played by the vortex sector of the theory for the square lattice, Fig. 8. When vortex configurations are not included in the Markov chain, the model can be mapped onto the SOS model and scaling is observed. On the other hand, when vortices are included, no scaling over a region of finite extent is observed.

Our susceptibility data are consistent with the theoretical picture of Fig. 2. For trajectories close to the SOS line it seems that the true divergent (and therefore scaling) behavior of χ occurs at a single temperature, reflected by a sharp peak in $\chi(T)$. The apparent scaling region above this peak is a crossover effect, due to the proximity of the trajectory to the SOS line, which does exhibit scaling behavior for $T>T_c$.

Our results can be summarized as follows:

(a) We find evidence for a single transition for both square and triangular cases.

(b) In the case of the triangular lattice, the transition takes place on the line calculated by Enting, as shown by the behavior of the susceptibility.

(c) For both lattices the specific heat of the model has two peaks for temperature trajectories in the region bounded by the decoupling and $X(180)=0$ lines. Between the Potts and decoupling lines, only one peak is observed.

(d) For the square lattice, the low-temperature peak of the specific heat falls on the self-dual line; thus we can associate it with the transition. On the other hand, the same peak in the triangular case does not follow the Enting line, and so we cannot associate it with the transition.

(e) For the triangular lattice, we find a very wide crossover region in the vicinity of the SOS line, on which the susceptibility definitely scales.

These results seem to be in accord with the two-phase picture of the model and thus confirm the universality of N_c. Nevertheless, they raise new questions concerning aspects of the $Z(4)$ model defined on a triangular lattice, such as the width of the crossover region mentioned above, and the appearance of the susceptibility maxima and low-temperature peaks in the specific heat at different temperatures for the triangular lattice, and at the same temperature for the square lattice.

ACKNOWLEDGMENTS

We thank B. Nienhuis for most helpful discussions. This work was supported by the U. S.-Israel Binational Science Foundation, Jerusalem, and an A. Dissentshik Career Development Chair (E.D.).

[1]For recent reviews and articles see M. N. Barber, Phys. Rep. 59, 375 (1980); F. Y. Wu, Rev. Mod. Phys. 54, 235 (1982); M. Schick, in *Phase Transitions in Surface Films,* edited by J. G. Dash and J. Ruvalds (Plenum, New York, 1979), p. 65; K. Binder, in Trends of Physics, Proc. EPA Gen. Conf., York 1979, p. 164; M. Kohmoto, M. den Nijs, and L. P. Kadanoff, Phys. Rev. B 24, 5229 (1981); L. P. Kadanoff and M. Kohmoto, Nucl. Phys. B 190 [FS3], 671 (1981).

[2]J. V. José, L. P. Kadanoff, S. Kirkpatrick, and D. R. Nelson, Phys. Rev. B 16, 1217 (1977).

[3]S. Elitzur, R. Pearson, and J. Shigemitsu, Phys. Rev. D 19, 3698 (1978).

[4]E. Domany and E. K. Riedel, Phys. Rev. Lett. 40, 561 (1978); M. P. M. den Nijs, M. P. Nightingale, and M. Schick (unpublished).

[5]J. M. Kosterlitz and D. J. Thouless, J. Phys. C 6, 1181 (1973).

[6]L. P. Kadanoff and A. C. Brown, Ann. Phys. 121, 318 (1979).

[7]L. P. Kadanoff, Ann. Phys. 120, 39 (1979).

[8]H. J. F. Knops, Ann. Phys. 128, 448 (1980).

[9]H. J. F. Knops and L. W. J. Den Ouden, Ann. Phys. 138, 155 (1982).

[10]E. Domany, D. Mukamel, and A. Schwimmer, J. Phys. A 13, L311 (1980).

[11]C. Fan, Phys. Lett. 39A, 136 (1972).

[12]F. J. Wegner, J. Phys. C 5, L131 (1971).

[13]R. J. Baxter, Phys. Rev. Lett. 26, 832 (1971).

[14]M. P. den Nijs, Phys. Rev. B 23, 6111 (1981).

[15]D. C. Mattis and E. L. Lieb, J. Math. Phys. 6, 304 (1965).

[16]E. Domany, D. Mukamel, B. Nienhuis, and A. Schwimmer, Nucl. Phys. B 190 [FS3], 279 (1981) and unpublished.

[17]M. Einhorn, R. Savit, and E. Rabinovici, Nucl. Phys. B 170 [FS1], 16 (1980).

[18]F. C. Alcaraz and R. Koberle, J. Phys. A 13, L147 (1980).

[19]R. Savit, Phys. Rev. B 22, 3443 (1980).

[20]I. G. Enting J. Phys. A 8, L5 (1975).

[21]F. Y. Wu, J. Phys. C 10, L23 (1977).

[22]D. J. Amit, Y. Y. Goldschmidt, and G. Grinstein, J. Phys. A 13, 585 (1980).

[23]M. E. Fisher and M. N. Barber, Phys. Rev. Lett. 28, 1516 (1972).